Journal of Magnetic Resonance 199 (2009) 166–172

Contents lists available at ScienceDirect

Journal of Magnetic Resonance

journal homepage: www.elsevier.com/locate/jmr

Spectral characterization of diffusion with chemical shift resolution: Highly concentrated water-in-oil emulsion

Samo Lasič *, Ingrid Åslund, Daniel Topgaard

Division of Physical Chemistry, Center of Chemistry and Chemical Engineering, Lund University, P.O. Box 124, S-221 00 Lund, Sweden

ARTICLE INFO

Article history:
Received 14 January 2009
Revised 20 April 2009
Available online 3 May 2009

Keywords:
Modulated gradient spin-echo
CPMG
Diffusion spectrum
Chemical shift
Restricted diffusion
Emulsion
Size distribution
Molecular exchange

ABSTRACT

We present a modulated gradient spin-echo method, which uses a train of sinusoidally shaped gradient pulses separated by 180° radio-frequency (RF) pulses. The RF pulses efficiently refocus chemical shifts and de-phasing due to susceptibility differences, resulting in undistorted, high-resolution diffusion weighted spectra. This allows for the simultaneous spectral characterization of the diffusion of several molecular species with different chemical shifts. The technique is robust against susceptibility artifacts, field inhomogeneity and imperfections in the gradient generating equipment. The feasibility of the technique is demonstrated by measuring the diffusion of water, oil, and water-soluble salt in a highly concentrated water-in-oil emulsion. The diffusion of water and salt reveal precise information about the droplet size distribution below the μm-range. Common droplet size distribution explains both the data for water with finite long-range diffusion and the data for salt with negligible long-range diffusion. The results of water diffusion show that the technique is efficient in deconvolving the effects of molecular exchange between droplets and restricted diffusion within droplets. The effects of water exchange suggest that droplets of different sizes are uniformly distributed within the sample.

1. Introduction

NMR diffusometry is a well-established approach to non-invasively study the morphology of porous materials and emulsions by characterization of self-diffusion in the interstitial fluid. For this purpose different methods have been developed. Most widely used methods consist of two short gradient pulses and are based on the displacement propagator formalism [1,2]. They rely on the short gradient pulse (SGP) approximation, which holds when the diffusive displacement of the spin-bearing particles during the application of a gradient pulse is much shorter than the extent of the confinements. Most commonly the pulsed field gradient (PFG) experiments aim to determine the mean square displacement occurring in the time interval between the two gradient pulses. Restricted environments give rise to a time-dependent diffusion coefficient, which can be probed by the PFG experiments and reveal morphological properties of porous materials, such as the pore size, surface-to-volume ratio, tortuosity and permeability [3–6]. The information about the pore size and shape can alternatively be obtained by determination of the average displacement propagator at a fixed diffusion time. Its Fourier transform can be measured by varying the reciprocal space vector q, which is defined by the strength and duration of the gradient pulses [7]. This approach takes advantage of diffraction-like effects on plots of echo intensity vs. q, which are related to the characteristic distances in the sample. To adequately probe small pores, the propagator has to be sampled at short diffusion times, which requires strong gradient pulses in order to achieve adequate signal attenuation. In addition, short pulses are required for the SGP approximation to be valid. The lowest limit of the length scales accessible by the PFG experiment is set by hardware limitations, i.e. gradient power restraints and eddy current artifacts. However, studies have been done in order to overcome the limits set by the SGP approximation. The effects of finite length gradient pulses in characterizing emulsions have been thoroughly examined [8] and brought into use [9]. Variable pulse duration can be used to determine the minimum length-scale for which diffusion appears to be Gaussian. Åslund et al. have shown that a controlled break down of the SGP approximation can be applied to determine the homogeneous length-scale of micro-heterogeneous systems such as lamellar liquid crystals [10].

Studies of emulsions are important due to implications in many technological applications but they are also often used as testing systems to establish new experimental methods. Packer and Rees where the first to apply the PFG method to study restricted diffusion in an emulsion [11]. Balinov et al. observed diffraction peaks in the attenuation data of a water-in-oil emulsion [12]. The PFG approach has been widely used to determine the droplet size distribution (DSD) in emulsions, which is an important characteristic influencing stability, rheology and functionality of emulsions. It is important to note that the migration of molecules between

* Corresponding author. Fax: +46 46 222 44 13.
E-mail addresses: samo.lasic@fkem1.lu.se, samo.lasic@fmf.uni-lj.si (S. Lasič).

1090-7807/$ - see front matter © 2009 Elsevier Inc. All rights reserved.
doi:10.1016/j.jmr.2009.04.014

droplets can severely limit the usefulness of the PFG approach to study emulsions. It has been clearly shown that when there is finite probability that molecules leave the droplet during the gradient pulse, diffusion appears Gaussian and the information about the droplet size is lost [8]. Furthermore, several authors in the literature have observed that the measured DSD depends on the diffusion time. The primary reason for this was attributed to molecular exchange between emulsion droplets (see review article [13]). While exchange is of scientific interest, it compromises the ability to quantitatively determine the DSD by PFG experiments.

Another approach to measure diffusion, which does not necessarily use pulsed gradients, is known as the modulated gradient spin-echo method (MGSE) [14–17]. It provides information about diffusion in the frequency domain. By generating a periodically oscillating phase factor, the MGSE experiment results in a signal attenuation which is proportional to the spectrum of the velocity auto-correlation function (VAF) of the spin-bearing particles. The effect of spin de-phasing due to diffusion is accumulated over many gradient modulation cycles, giving rise to adequate diffusive attenuation on a shorter time scale compared to the PFG method. The diffusion spectrum, probed by MGSE, is related to the mean square displacement and, analogously to the time-dependent diffusion coefficient, contains information about the morphology [18]. Its zero frequency component corresponds to the long range diffusion, while higher frequency components approach the bulk diffusion value. Different kinds of MGSE experiments have been employed to study water diffusion in porous media [19] and in emulsions [20], but without chemical shift resolution. Parsons et al. have implemented harmonically oscillating gradients, which are compatible with imaging sequences [21]. Oscillating gradients were successfully used to probe diffusion in rat brain [22]. It has been shown that such an approach can be used to decompose disperse flow and restricted diffusion, determine pore sizes, surface-to-volume ratios and tortuosity [23,24].

Here we present an application of the MGSE method, which uses sinusoidally shaped gradient pulses separated by 180° RF pulses. This produces an apodized cosine effective gradient waveform, similar to the one used in [21–23]. The RF pulses used in the presented technique efficiently refocus chemical shifts and dephasing due to susceptibility differences, resulting in undistorted, high-resolution diffusion weighted spectra. While measurements of individual components in solution by the spin-echo PFG technique [25] are well established, the experiment described herein is the first MGSE approach that, to our knowledge, yields chemical shift resolution. The MGSE experiment was employed to study the diffusion of different species in a highly concentrated water-in-oil emulsion. Such emulsions were previously studied by PFG [8,9,26]. In order to access diffusion on a shorter time scale, an MGSE approach with a train of gradient pulses was applied to the same emulsion system [20]. However, the eddy currents produced by these sharp gradient pulses compromised the chemical shift resolution. The high-resolution diffusion weighted spectra obtained by the novel MGSE technique allows the diffusion of different species to be studied within the same experiment and reveal identical DSD from species with both finite and negligible long-range diffusion.

2. Theory

2.1. Background

If the relaxation effects are factored out, the normalized echo intensity at the time of echo acquisition t_e is given by the ensemble average $E(t_e) = \langle \exp(i \int_0^{t_e} \omega(t)\, dt) \rangle$, where $\omega(t) = \gamma G(t) x(t)$. Here γ is the gyromagnetic ratio, $G(t)$ is the effective gradient waveform and $x(t)$ is the particle position along the gradient direction. The ensemble average can be expressed by the cumulant expansion and in the Gaussian approximation the signal is written in terms of the signal phase ϕ and the attenuation factor β as $E = e^{i\phi-\beta}$. As the MGSE method relies on the rate of the gradient modulation rather than on its magnitude, the size of the confinement can always be smaller than the spin phase grating created by the applied gradient, and the signal analysis within the Gaussian approximation is valid [27]. While the signal phase is proportional to the net flow, the attenuation is influenced by the diffusion process [14]. Stepišnik and Callaghan have shown that the attenuation factor can be expressed in the frequency domain [14–16]. In the direction along the applied gradient the expression can be written as

$$\beta = \frac{1}{\pi} \int_0^\infty |F(\omega)|^2 D(\omega)\, d\omega. \tag{1}$$

Here $D(\omega)$ is the spectrum of the VAF, also called the diffusion spectrum, and $F(\omega) = \int_0^{t_e} F(t) e^{i\omega t}\, dt$ is the spectrum of the phase factor, which is determined by the effective gradient waveform $F(t) = \gamma \int_0^t G(t')\, dt'$. It follows from Eq. (1) that separate frequency components of the diffusion spectrum can be measured if the spectrum of the phase factor $F(\omega)$ has a narrow frequency peak at a non-zero frequency. This is achieved in MGSE experiments by an appropriate choice of the gradient modulation waveform. When $F(\omega)$ has no zero-frequency component, the experiment is flow compensated, as the phase of the signal is proportional to the product of the flow velocity and the 0th moment of the phase factor $\int_0^{t_e} F(t)\, dt$ [14].

The diffusion spectrum can be interpreted as a frequency domain counterpart of the time-dependent diffusion coefficient $D_t(t) = \langle \Delta x^2 \rangle / 2t$. The two are connected through the mean square displacement, which can be expressed as

$$\langle \Delta x(t)^2 \rangle = \frac{4}{\pi} \int_0^\infty \frac{D(\omega)}{\omega^2} (1 - \cos \omega t)\, d\omega. \tag{2}$$

An analytical expression for the restricted diffusion spectrum $D(\omega)$ can be derived for simple geometries (planar, cylindrical, spherical) from the appropriate propagators like it is done in cases of time-domain experiments, where the time-dependent diffusion coefficient is of interest. See for example the derivation of Murday and Cotts for the apparent diffusion coefficient in spherical geometry measured by the spin-echo PFG experiment [28]. A convenient way to obtain $D(\omega)$ is to derive an expression for the mean square displacement $\langle \Delta x(t)^2 \rangle$, calculate the VAF as $\langle v(t) v(0) \rangle = \frac{1}{2} \frac{d^2}{dt^2} \langle \Delta x(t)^2 \rangle$ and finally Fourier transform it into the frequency domain. Such a derivation is provided by Stepišnik in [18]. Here we sum up the results for $D(\omega)$ for planar, cylindrical and spherical geometry in a more compact form. With the addition of tortuosity term [19] the diffusion spectrum can be written as

$$D(\omega) = \alpha D_0 + (1 - \alpha) D_0 \sum_{k=1}^{\infty} \frac{a_k B_k \omega^2}{a_k^2 D_0^2 + \omega^2}, \tag{3}$$

where $\alpha = D_\infty / D_0$ is the inverse tortuosity, the ratio between the long-range diffusion D_∞ and the short-range diffusion D_0. The coefficients a_k and B_k depend on the geometry under consideration and can be expressed as

$$a_k = \left(\frac{\zeta_k}{R} \right)^2, \tag{4a}$$

$$B_k = \frac{2(R/\zeta_k)^2}{\zeta_k^2 + 1 - d}, \tag{4b}$$

where ζ_k are the kernels of

$$\zeta J_{d/2-1}(\zeta) - (d-1) J_{d/2}(\zeta) = 0 \tag{5}$$

and J_ν denotes the νth order Bessel function of the first kind. The coefficient d is set to 1, 2 or 3 for planar, cylindrical or spherical geometries, respectively, and $2R$ is the plane spacing or the diameter of the pore.

2.2. Experimental technique

The pulse sequence consists of a CPMG RF train with $2N$ 180° pulses and interspaced gradient pulses with sinusoidal shape (Fig. 1). Only half of the last echo is acquired at a fixed echo time $t_e = NT_m$, where N is the number of modulation periods and T_m is the modulation period. The refocusing pulses are separated by $T_m/2$. The shape of the gradient pulses is defined by $G_0 \sin(\omega_m t)$, where $\omega_m = 2\pi/T_m$ is the modulation frequency. Note that the first and the last pulse in the sequence oscillate with the double modulation frequency. The corresponding effective gradient $G(t)$ has an apodized cosine shape (Fig. 2A) and the phase factor oscillates periodically around zero with the modulation period T_m (Fig. 2B).

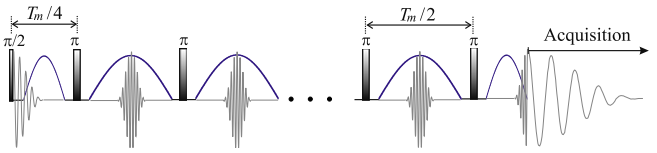

Fig. 1. Schematic timeline of an RF pulse sequence with sinusoidal gradient lobes. The refocusing pulses are repeated with the period $T_m/2$. Sketched is also the evolution of the magnetization.

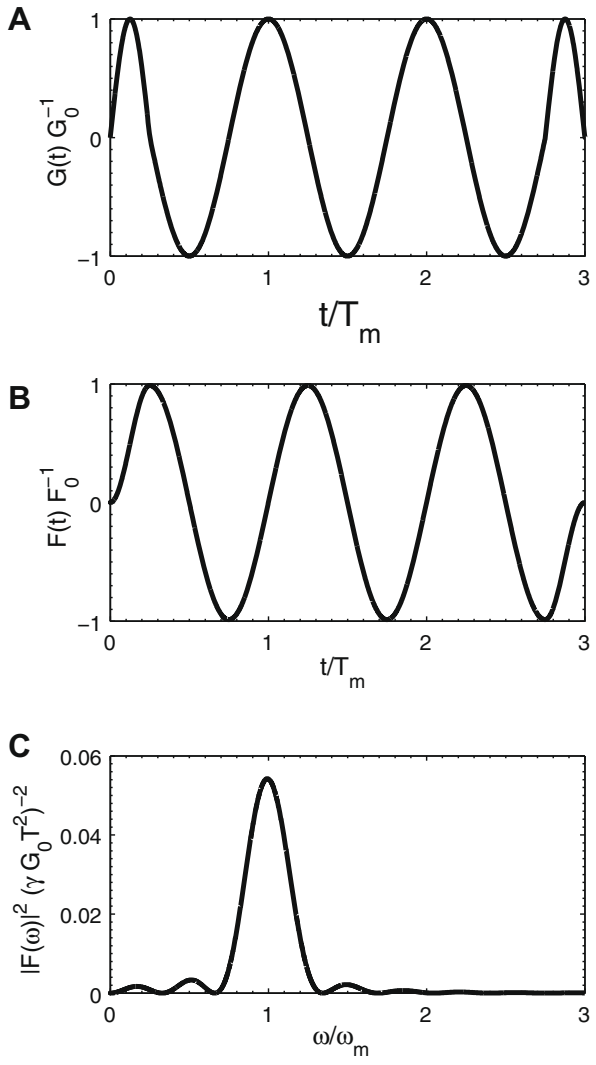

Fig. 2. Gradient modulation with $N = 3$ modulation periods. (A) Effective gradient, (B) phase factor, and (C) Spectrum of the phase factor.

The amplitude of the phase factor is $F_0 = \frac{1}{2\pi}\gamma G_0 T_m$. The spectrum of the phase factor has a peak centered around ω_m with the width inversely proportional to t_e (Fig. 2C). The spectrum of the phase factor can be written as a function of normalized frequency $\tilde{\omega} = \omega/\omega_m$ as

$$\frac{|F(\tilde{\omega})|}{(\gamma G_0 T_m^2)} = \left[(2+\tilde{\omega}^2)\cos\left((N-1/2)\pi\tilde{\omega}\right) + 2(\tilde{\omega}^2-1)\cos(\pi N\tilde{\omega})\right] / \left[2\pi^2\tilde{\omega}(1-\tilde{\omega}^2)(4-\tilde{\omega}^2)\right]. \quad (6)$$

When the pulse sequence consists of several modulation periods the attenuation can be approximated as $\beta(\omega) \approx bD(\omega)$, where b is the attenuation factor

$$b = \left(\frac{\gamma G_0}{8\pi}\right)^2 t_e^3 \frac{8N-1}{N^3}. \quad (7)$$

In order to sample the diffusion spectrum, the modulation period T_m and the number of periods N are varied. As the echo time t_e is kept constant, in order to avoid relaxation effects, the set of sampled frequencies at a chosen t_e is bound to $\omega_m = 2\pi N/t_e$. The lowest modulation frequency that can be probed is limited by T_2 relaxation, while the upper limit is set by the gradient slew rate. The choice of performing the experiment at a constant t_e also factors out possible J-coupling effects, which are not refocused by the 180° pulses. However, t_e should be chosen carefully, to optimize S/N, when J-coupling effects are present.

3. Experimental

3.1. Materials and emulsion preparation

We studied a highly concentrated water-in-oil emulsion, which consists of 95 wt% 0.2 M tetramethyl ammonium chloride (TMA-Cl) in Millipore water as aqueous phase, 3.5 wt% heptane as oil phase and 1.5 wt% Brij 92 as surfactant. The ingredients and sample preparation were the same as reported in [8]. We used the surfactant Brij 92 from Aldrich, heptane of p.a. quality from Merck and TMA-Cl from Fluka Biochemica. The surfactant was dissolved in oil in a glass tube containing several glass beads. The water was then added drop-wise while shaking the sample on a vortex-mixer. When the emulsion became viscous additional shaking was done by hand. Previous experiments have shown that this type of emulsion is stable for at least 15 h [8,26].

3.2. NMR experiment

The experiment was performed at 200.13 MHz proton resonance frequency on a Bruker AVII-200 spectrometer. A Bruker DIFF-25 probe and a Bruker GREAT 1/40 gradient amplifier were used, providing a magnetic field gradient in the z-direction with a maximum strength of 9.6 T/m. No gradient blanking was used between subsequent gradient pulses. The 180° pulse length was 24 μs and the separation between the RF pulses and the gradient pulses was 10 μs. The time between the gradient pulses (Fig. 1) was thus 44 μs, which had a negligible effect on the calculation of b values in our experiment. In order to factor out the relaxation effects the experiment was performed with constant $t_e = 150$ ms. Diffusion was probed at 36 different modulation frequencies. At each T_m, between 2 ms and 30 ms, the number of modulation periods was adjusted so that $t_e = NT_m$. The corresponding N were between 5 and 75 incremented by 2. The gradient amplitude was adjusted so that the same 20 linearly stepped b values were applied at each modulation period. The maximum gradient amplitude, used at the shortest T_m, was 2.9 T/m. The standard 8 steps CPMG phase cycling was applied. Measurements were done at 25 °C. With an acquisition time of 1 s and a recycle delay of 1 s

the whole experiment with 36×20 spectra measured was performed in approximately 3.44 h.

4. Results and discussion

The experiment gives spectra with high chemical shift resolution. Thus, it allows diffusion of different molecules to be measured within a single experiment. Fig. 3A depicts the emulsion spectrum attenuated by diffusion at $T_m = 2$ ms. Water, TMA and oil peaks are clearly resolved. In Fig. 3B one can see that the spectral resolution of our experiment is comparable to the spectrum of the free-induction decay (FID) with 8 scans. The relative differences between the peak intensities in Fig. 3B are caused by differences in the relaxation times. The intensities of the separate peaks were analyzed in terms of Stejskal–Tanner plots.

The method was tested by measuring bulk diffusion of water, methanol, glycerin and octanol (data not included here). The diffusion spectra were flat as expected. However, at modulation frequencies above 700 Hz the echo attenuation increases rapidly, which can be attributed to residual gradients leading to slice selection with the refocusing pulses. To avoid this effect we set the upper frequency limit of our experiment to 500 Hz. The same limit was achieved by Topgaard et al. [20] in a MGSE experiment with a train of rectangular gradient pulses. Interestingly, the same equipment was used in both cases except that the gradient coil was driven by a Bruker BAFPA-40 instead of a newer Bruker GREAT 1/40 amplifier.

As a reference the bulk diffusion of water and TMA^+ ions in the TMA-Cl solution used in the preparation of the emulsion were measured with the same experimental parameters as the emulsions. The diffusion spectrum of both species is flat as expected (Fig. 4). Within 5% of accuracy the respective values for TMA^+ and water are 1.0×10^{-9} m^2/s and 2.3×10^{-9} m^2/s. These values are used as the bulk limit D_0 in the diffusion model fitted to the emulsion data. A small but systematic decrease of the diffusion at increasing frequencies can be observed for the dominant water peak (Fig. 4A). This effect has been noted also by others [15,20] and can probably be attributed to the effects of coil impedance leading to slightly reduced b values at larger ω_m.

In the emulsion, diffusion of oil, water and TMA^+ ions has distinctively different characters. The water droplets, in which TMA-Cl is dissolved, are very tightly packed [8,29]. The oil is diffusing in a thin film surrounding the droplets. Water molecules are partially soluble in oil and can migrate between droplets. On the other hand, the solubility of TMA^+ is negligible, thus the ions are completely confined within the droplets. During the experiment water molecules can diffuse across the droplet space several times before leaving the droplet. Their diffusion exhibits clear frequency dependence characteristic of restricted diffusion (Fig. 5). One can also see that due to water migration between droplets the data approach to a finite value of D_∞ at low frequencies. The data in Fig. 5 is obtained from exponential fits of the decay curves in the Stejskal–Tanner plot. For clarity Fig. 6A depicts the decay curves only at selected modulation frequencies. The error bars in Fig. 5, as well as in Figs. 4 and 7, are obtained by means of Monte Carlo analysis similar to the one described in [30] and indicate confidence intervals of 80%. The diffusion spectrum of water cannot be fitted by the theoretical model for spherical geometry of a single size (Eq. (3)). The situation is clarified when the diffusion of TMA^+ is considered. In contrast to

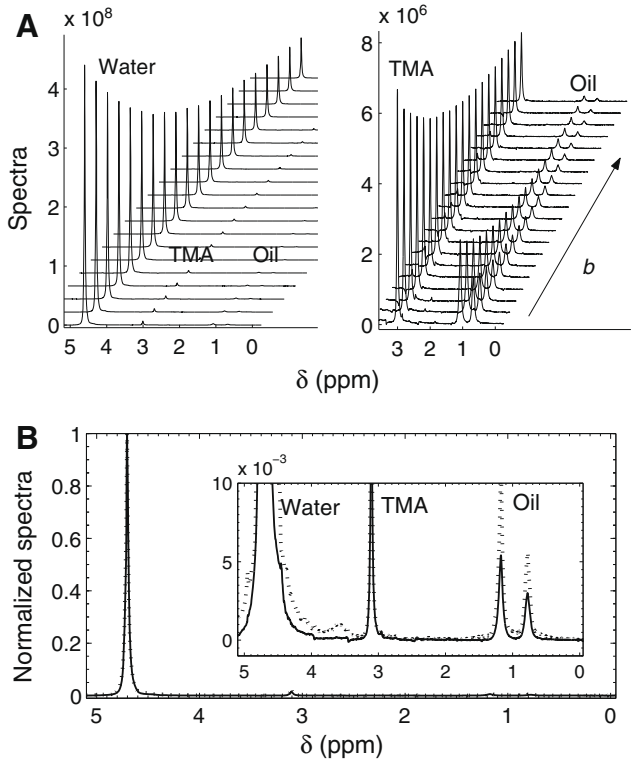

Fig. 3. (A) Diffusive attenuation of the emulsion spectrum at $T_m = 2$ ms. The spectrum consists of water, TMA and oil peaks. On the right-hand side is a close up of TMA and oil peaks. The arrow indicates linearly increasing b values. (B) Comparison of the FID spectrum (dotted line) and the spin-echo spectrum (solid line) at $T_m = 2$ ms and lowest gradient amplitude ($b = 2 \times 10^8$ s/m^2). The acquisition time was 1 s and the dwell time 200 μs. The spectra are normalized with respect to the maximum intensity of the FID spectrum. The intensity range is 100× reduced in the inset figure.

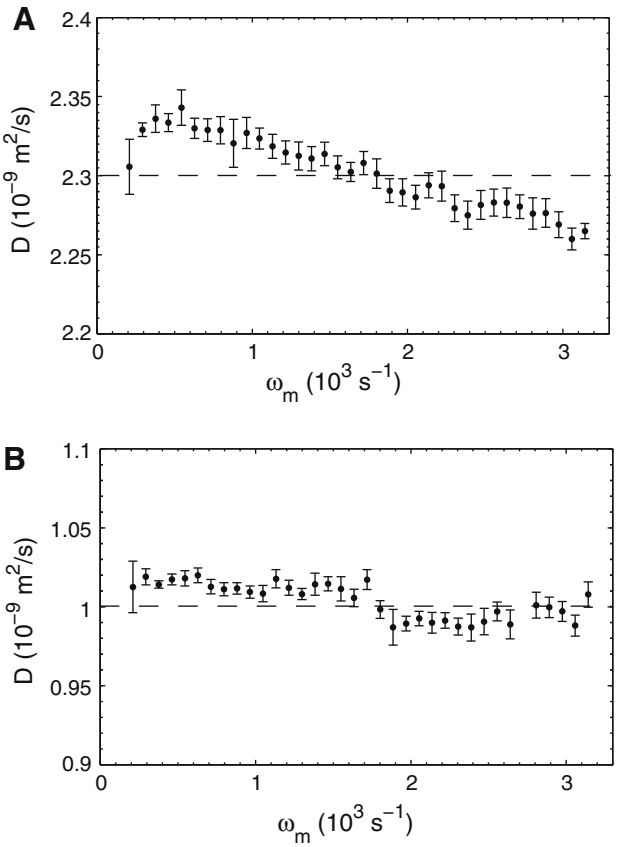

Fig. 4. Diffusion spectrum of water (A) and TMA^+ ions (B) in solution. The dashed line indicates the mean value and the error bars indicate confidence intervals of 80%.

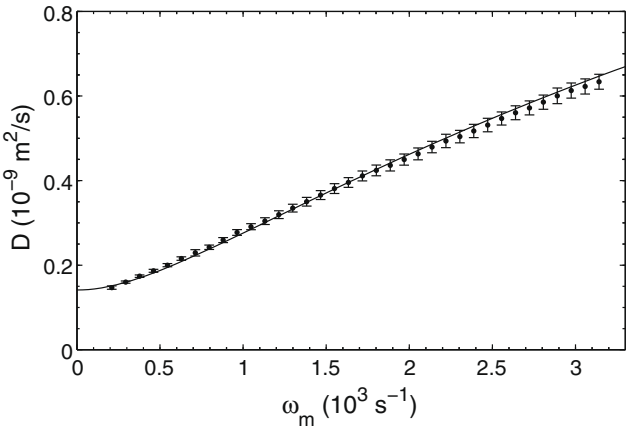

Fig. 5. Diffusion spectrum for water (dots) and the theoretical model (solid line). Error bars indicate confidence intervals of 80%.

Fig. 6A one can see that the decay curves for TMA depicted in Fig. 6B are not single exponential. Note that the *b*-values used in our experiment (see Fig. 6A) were sufficiently low for the Gaussian approximation of cumulant expansion to be valid [27] for restrictions in the assumed μm size range (see Fig. 6C). In a single compartment the decay curves would be mono-exponential. We have verified this by simulating the MGSE experiment results in a 1D periodic system of permeable pores, where diffusion was simulated by means of finite-difference method of integration of the Bloch–Torrey equation. The same simulation method was used in [10] and is described therein. The multi-exponential decay curves for TMA thus suggest that the droplets are poly-disperse in size. The same poly-dispersity also explains the shape of the diffusion spectrum of water (Fig. 5).

Although the diffusion of water and TMA^+ appear to be very different it shares the same morphological information. We model the data by assuming a log-normal probability density for the DSD, which is given by

$$P(R) = \frac{1}{\sqrt{2\pi}\sigma R}\exp\left[-\frac{(\ln R - \ln \mu)^2}{2\sigma^2}\right], \tag{8}$$

where μ is the median and σ is the width of the distribution. There is abundant experimental evidence that such a distribution describes well the poly-dispersity of the droplet size in a broad range of emulsion systems [11,13,31]. In the case of TMA^+ ions, the spins which are confined to droplets of different size, contribute differently to the attenuation of the echo intensity. It can be written as a weighted sum

$$E(\omega_m) = \sum_R P_V(R)\, e^{-bD(R,\omega_m)}. \tag{9}$$

By P_V we denote the normalized volume based distribution, to distinguish it from its number based counterpart P_N. The two distributions are related by $P_V = P_N(R)R^3/\sum_R P_N(R)R^3$ and both have the log-normal shape (8). The corresponding medians are related by $\mu_V = \mu_N e^{3\sigma^2}$ and the mean value is provided by $\langle R\rangle = \mu e^{\sigma^2/2}$.

In the case of water the situation is quite different. Due to the exchange of molecules, the signal originating from different parts of the sample, i.e. droplets of different size, exhibit equal diffusive attenuation. In this case the decay is mono-exponential

$$E(\omega_m, \alpha) = e^{-bD_{\mathrm{mix}}(\omega_m,\alpha)}. \tag{10}$$

Such a situation takes place if molecules roam over all characteristic droplets in the system during t_e.

Consider the probability density $p_{\mathbf{r}}(R)$ to find a molecule at position $\mathbf{r}$ at the time t_e, if it was within a droplet of size R at the beginning

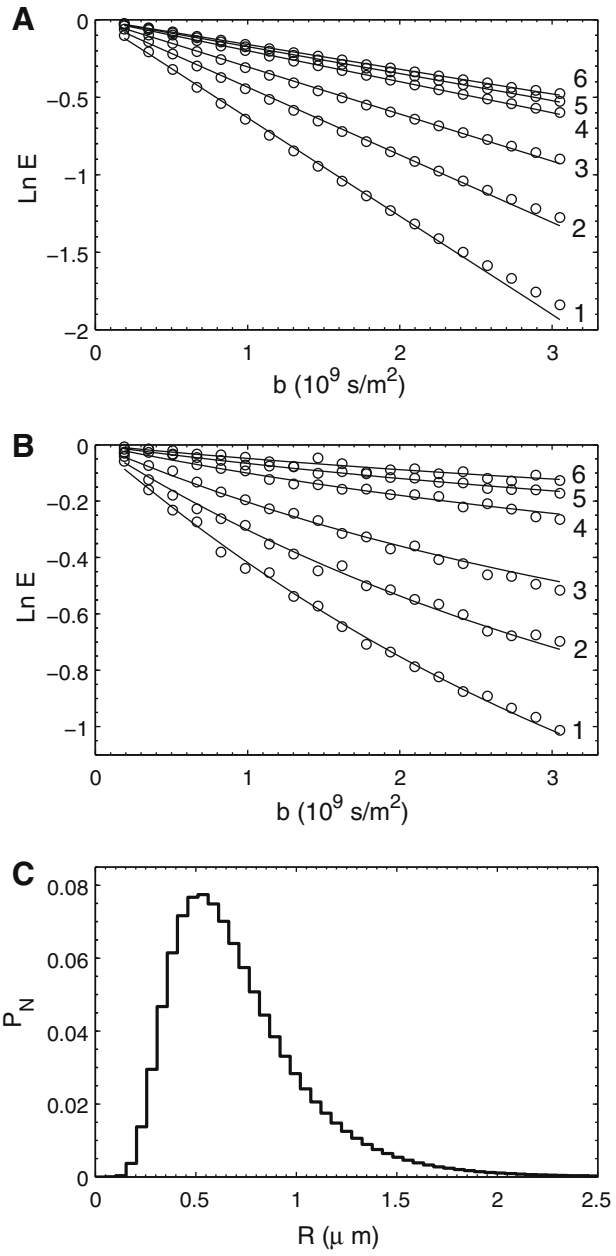

Fig. 6. Echo intensity decay of water (A) and TMA (B) peaks at selected modulation periods (circles). Labelled 1–6 are T_m = 2, 3.3, 5.5, 11.5, 16.7 and 21.4 ms corresponding to N = 75, 45, 27, 13, 9 and 7 modulation periods. Solid lines in A and B correspond to the theoretical model with the common log-normal DSD (C).

of the experiment. Note that $p_{\mathbf{r}}(R)$ depends on t_e and it should not be confused with the droplet size distributions P_N or P_V. When there is no molecular exchange between droplets $p_{\mathbf{r}}(R)$ is zero everywhere except for $\mathbf{r}$ within droplets of size R. In this case there are different contributions to the diffusive attenuation, resulting in multi-exponential decay described by Eq. (9). However, when there is enough molecular exchange between droplets during t_e the probability density $p_{\mathbf{r}}(R)$ is independent of position. Signal originating from different parts of the sample is thus equally attenuated. In this case all the spins belong to the statistical ensemble described by a common average VAF. It can be written as a sum over sub-ensembles of spins originating in droplets of different sizes. Thus, the average diffusion spectrum is given by

$$D_{\mathrm{mix}}(\omega_m, \alpha) = \sum_R P_V(R) D(R, \omega_m, \alpha). \tag{11}$$

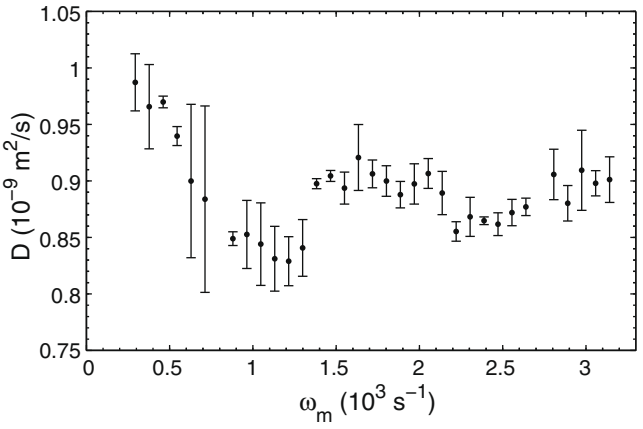

Fig. 7. Diffusion spectrum of oil. Error bars indicate confidence intervals of 80%.

Note that in this case α is not zero. The mono-exponential decay of water intensities (Fig. 6A) suggests that the droplets of different sizes are evenly distributed within the sample. If there would be large domains (>20 μm) of droplets with different sizes, the decay of water intensity would not be mono-exponential.

A global fit of the volume-based log-normal size distribution (8) to the water and TMA data (Fig. 6A and B) was performed in terms of Eqs. (9) and (10). The distribution was represented by 50 linearly spaced bins between 0 and 2.5 μm. The fitting comprised $2 \times 36 \times 20$ data points and yields parameters μ_V, σ and α. This corresponds to the resulting theoretical curves, depicted in Figs. 5 and 6A and B. In order to estimate the fitting error, the Monte Carlo procedure was performed in a manner similar to that described in the work of Balinov et al. [31], where the DSD in an emulsion was measured by the spin-echo PFG experiment. Within 80% of confidence the obtained fitting parameters are $\mu_V = 1.217 \pm 0.0075$ μm, $\sigma = 0.475 \pm 0.018$ and $\alpha = 6.75 \pm 0.35\%$. The same fitting procedure was performed using the number-based distribution (Fig. 6C) yielding equal σ and α but $\mu_N = 0.619 \pm 0.031$ μm. The fact that the experiment is sensitive to volume rather than to number weighting is reflected by a smaller relative error of about 0.6% in case of μ_V compared 5% error for μ_N. The estimated mean droplet size according to μ_N is $\langle R \rangle = 0.785$ μm. The long-range diffusion value $D_\infty \approx 1.5 \times 10^{-10}$ m^2/s and the mean droplet size are in good agreement with previously obtained results [20,26].

As expected, in the case of oil diffusion the $D(\omega)$ is flat in the observed frequency range (Fig. 7). In this case the fluctuation of the measured data, within 7%, is larger due to the low volume fraction of oil and consequently lower signal-to-noise ratio. The diffusion of oil (heptane) is seen to be hindered by the droplets. The tortuous diffusion paths of heptane molecules result in diffusion rate of about 0.9×10^{-9} m^2/s, which is about 30% of the heptane bulk value (3.12×10^{-9} m^2/s).

5. Conclusions

The MGSE technique which enables spectral characterization of diffusion with chemical shift resolution is introduced. The use of spin echoes instead of gradient echoes [21] is advantageous in reducing the effects of field inhomogeneity and susceptibility artifacts. Many modulation periods can be used, thus high sensitivity at short times can be achieved. The smooth gradient modulation results in reduced eddy currents and high resolution spectra. As the polarity of the gradient pulses is not switched, the effect of asymmetry of the gradient pulses with opposite polarity is avoided, which can be significant in the case of gradient-echo experiments. The technique is particularly suited for in vitro studies of samples where diffusion of several compounds, with different chemical shifts, is of interest.

The potential of the presented technique is demonstrated by studying a highly concentrated water-in-oil emulsion. The results are in good agreement with previous studies of similar systems [20,26] but reveal additional and more detailed information. Within a single experiment the diffusion of water, TMA^+ ions and oil can be studied. Diffusion of the continuous oil phase is seen to be Gaussian but hindered. The ions, which are confined to the droplets, shows restricted diffusion behavior with infinite tortuosity ($D_\infty = 0$). The diffusion spectrum of water reveals both the value of D_∞ due to migration of molecules between droplets and the information about restrictions. Due to size poly-dispersity the TMA intensities decay multi-exponentially, while migration of water result in mono-exponential decays. The two distinct diffusive behaviors can be appropriately modelled and fit well to a common DSD. This provides reliable size distribution parameters. Furthermore, it leads to the conclusion that droplets of different sizes are uniformly distributed within the sample. The results confirm that in MGSE experiments the effects of molecular exchange can be efficiently deconvolved from restricted diffusion, in contrast to PFG experiments in which exchange can hinder information about droplet size [8,9] and inhibit the ability of precise quantitative determination of the DSD [13].

Acknowledgments

This work is financially supported by the Crafoord Foundation, the Swedish Research Council (VR) and the Swedish Foundation for Strategic Research (SSF). Fruitful discussions with Olle Söderman and Janez Stepišnik are gratefully acknowledged.

References

[1] E.O. Stejskal, Use of spin echoes in a pulsed magnetic-field gradient to study anisotropic, restricted diffusion and flow, J. Chem. Phys. 43 (1965) 3597–3603.
[2] J. Kärger, W. Heink, The propagator representation of molecular transport in microporous crystallites, J. Magn. Reson. 51 (1983) 1–7.
[3] P.P. Mitra, P.N. Sen, L.M. Schwartz, Short-time behavior of the diffusion coefficient as a geometrical probe of porous media, Phys. Rev. B 47 (14) (1993) 8565–8574.
[4] L.L. Latour, P.P. Mitra, R.L. Kleinberg, C.H. Sotak, Time-dependent diffusion coefficient of fluids in porous media as a probe of surface-to-volume ration, J. Magn. Reson. A 101 (1993) 342–346.
[5] M.D. Hürlimann, K.G. Helmer, L.L. Latour, C.H. Sotak, Restricted diffusion in sedimentary rocks: determination of surface-area-to-volume ratio and surface relaxivity, J. Magn. Reson. A 111 (1994) 169–178.
[6] P.N. Sen, Time-dependent diffusion coefficient as a probe of the permeability of the pore wall, J. Chem. Phys. 119 (18) (2003) 9871–9876.
[7] P.T. Callaghan, D. MacGowan, K.J. Packer, F.O. Zelaya, High resolution q-space imaging in porous structures, J. Magn. Reson. 90 (1990) 177–182.
[8] C. Malmborg, D. Topgaard, O. Söderman, NMR diffusometry and the short gradient pulse limit approximation, J. Magn. Reson. 169 (2004) 85–91.
[9] C. Malmborg, M. Sjöbeck, S. Brockstedt, E. Englund, O. Söderman, D. Topgaard, Mapping the intracellular fraction of water by varying the gradient pulse length in q-space diffusion MRI, J. Magn. Reson. 180 (2006) 280–285.
[10] I. Åslund, C. Cabaleiro-Lago, O. Söderman, D. Topgaard, Diffusion NMR for determining the homogeneous length-scale in lamellar phases, J. Phys. Chem. B 112 (2008) 2782–2794.
[11] K.J. Packer, C. Rees, Pulsed NMR studies of restricted diffusion, J. Colloid Interface Sci. 40 (1972) 206–218.
[12] B. Balinov, O. Söderman, J.C. Ravey, Diffraction-like effects observed in the PGSE experiment when applied to a highly concentrated water/oil emulsion, J. Phys. Chem. 98 (2) (1994) 393–395.
[13] M.L. Johns, K.G. Hollingsworth, Characterisation of emulsion systems using NMR and MRI, Prog. Nucl. Magn. Reson. Spectrosc. 50 (2007) 51–70.
[14] J. Stepišnik, Measuring and imaging of flow by NMR, Prog. Nucl. Magn. Reson. Spectrosc. 17 (1985) 187–209.
[15] P.T. Callaghan, J. Stepišnik, Frequency-domain analysis of spin motion using modulated gradient NMR, J. Magn. Reson. A 117 (1995) 118–122.
[16] P.T. Callaghan, J. Stepišnik, Generalized analysis of motion using magnetic field gradients, Adv. Magn. Opt. Reson. 19 (1996) 325–388.
[17] J. Stepišnik, A new view of the spin echo diffusive diffraction in porous structures, Europhys. Lett. 60 (2002) 453–459.

[18] J. Stepišnik, Time-dependent self-diffusion by NMR spin-echo, Physica B 183 (1993) 343–350.
[19] J. Stepišnik, S. Lasič, A. Mohorič, I. Serša, A. Sepe, Spectral characterization of diffusion in porous media by the modulated gradient spin echo with CPMG sequence, J. Magn. Reson. 182 (2006) 195–199.
[20] D. Topgaard, C. Malmborg, O. Söderman, Restricted self-diffusion of water in a highly concentrated W/O emulsion studied using modulated gradient spin-echo NMR, J. Magn. Reson. 156 (2002) 195–201.
[21] E.C. Parsons, M.D. Does, J.C. Gore, Modified oscillating gradient pulses for direct sampling of the diffusion spectrum suitable for imaging sequences, Magn. Reson. Imaging 21 (2003) 279–285.
[22] M.D. Does, E.C. Parsons, J.C. Gore, Oscillating gradient measurements of water diffusion in normal and globally ischemic rat brain, Magn. Reson. Med. 49 (2003) 206–215.
[23] E.C. Parsons, M.D. Does, J.C. Gore, Temporal diffusion spectroscopy: theory and implementation in restricted systems using oscillating gradients, Magn. Reson. Med. 55 (2006) 75–84.
[24] P.T. Callaghan, S.L. Codd, Flow coherence in a bead pack observed using frequency domain modulated gradient NMR, Phys. Fluids 13 (2001) 421–427.
[25] P.T. Callaghan, C.M. Trotter, K.W. Jolley, A pulsed field gradient system for a Fourier transform spectrometer, J. Magn. Reson. 37 (1980) 247–259.
[26] C. Malmborg, D. Topgaard, O. Söderman, Diffusion in an inhomogeneous system: NMR studies of diffusion in highly concentrated emulsions, J. Colloid Interface Sci. 263 (2003) 270–276.
[27] J. Stepišnik, Validity limits of Gaussian approximation in cumulant expansion for diffusion attenuation of spin echo, Physica B 270 (1999) 110–117.
[28] J.S. Murday, R.M. Cotts, Self-diffusion coefficient of liquid lithium, J. Chem. Phys. 48 (11) (1968) 4938–4945.
[29] B. Håkansson, R. Pons, O. Söderman, Structure determination of a highly concentrated W/O emulsion using pulsed-field-gradient spin-echo nuclear magnetic resonance "diffusion diffractograms", Langmuir 15 (1999) 988–991.
[30] P. Stilbs, Fourier transform pulsed-gradient spin-echo studies of molecular diffusion, Progr. Nucl. Magn. Reson. Spectrosc. 19 (1987) 1–45.
[31] B. Balinov, O. Urdahl, O. Söderman, J. Sjöblom, Characterization of water-in-crude oil emulsions by the NMR self-diffusion techique, Colloids Surf. A 82 (1994) 173–181.